

KELVIN–HELMHOLTZ STABILITY CRITERIA FOR STRATIFIED FLOW: VISCOUS VERSUS NON-VISCOUS (INVISCID) APPROACHES

D. BARNEA and Y. TAITEL

Department of Fluid Mechanics and Heat Transfer, Faculty of Engineering, Tel-Aviv University,
Ramat-Aviv 69978, Israel

(Received 1 June 1992; in revised form 15 March 1993)

Abstract—The neutral stability lines obtained from the viscous Kelvin–Helmholtz analysis and the inviscid analysis are quite different for the case of low liquid viscosities, whereas they are quite similar for high viscosity, contrary to what one would expect. This puzzling result is considered in this work. It is shown that the stability behavior regarding the amplification rate is actually almost the same for the two analyses for a wide range of liquid viscosities and for various pipe inclinations. The results obtained in the present work also support Barnea's interpretation of the viscous and inviscid analyses as a means for predicting various transitions from stratified flow.

Key Words: stratified flow, stability, Kelvin–Helmholtz, flow pattern

INTRODUCTION

Kelvin–Helmholtz (KH) linear stability has been used frequently in the past for determining whether a smooth stratified flow is stable or unstable. Two types of KH analyses have been used: (1) The viscous Kelvin–Helmholtz (VKH) analysis, which uses the full two-fluid model and takes into account the shear stresses (Wallis 1969; Lin & Hanratty 1986; Wu *et al.* 1987; Andritsos *et al.* 1989; Barnea 1991; Crowley *et al.* 1992); and (2) the inviscid Kelvin–Helmholtz (IKH) theory, in which the shear stresses are neglected (Taitel & Dukler 1976; Kordyban 1977; Kordyban & Ranov 1970; Mishima & Ishii 1980). One would expect that the inviscid theory would be a good approximation for liquid of low viscosity, whereas for high viscosities one will have to use the full two-fluid model in order to get correct results. Surprisingly the results are just the opposite. For liquid of high viscosity the results of the IKH theory are applicable, while there is a large discrepancy in the results for the stability criterion between the IKH and VKH theories for low liquid viscosity.

This fact is demonstrated in figure 1. In this figure the neutral stability lines are plotted on a U_{LS} vs U_{GS} map to show the regions where stratified flow is stable or unstable. Both theories are used, the VKH theory and the IKH theory. As can be seen, for high viscosities the stability criteria using the aforementioned theories are almost identical, whereas for low viscosity they are quite different.

This dilemma motivated this work.

ANALYSIS

The stability analysis of stratified flow is performed on the “two-fluid model” equations. A brief outline of this analysis follows.

The continuity equations for the liquid and the gas are:

$$\frac{\partial}{\partial t} (\rho_L A_L) + \frac{\partial}{\partial x} (\rho_L A_L U_L) = 0 \quad [1]$$

and

$$\frac{\partial}{\partial t} (\rho_G A_G) + \frac{\partial}{\partial x} (\rho_G A_G U_G) = 0. \quad [2]$$

The momentum equations for each phase are:

$$\frac{\partial}{\partial t} (\rho_L A_L U_L) + \frac{\partial}{\partial x} (\rho_L A_L U_L^2) = -\tau_L S_L + \tau_i S_i - A_L \frac{\partial P_{iL}}{\partial x} - \rho_L A_L g \cos \beta \frac{\partial h_L}{\partial x} - \rho_L A_L g \sin \beta \quad [3]$$

and

$$\frac{\partial}{\partial t} (\rho_G A_G U_G) + \frac{\partial}{\partial x} (\rho_G A_G U_G^2) = -\tau_G S_G - \tau_i S_i - A_G \frac{\partial P_{iG}}{\partial x} - \rho_G A_G g \cos \beta \frac{\partial h_L}{\partial x} - \rho_G A_G g \sin \beta. \quad [4]$$

In the above, A is the cross-sectional area, h is the liquid level or gas gap, P is the pressure, U is the axial average velocity, τ is the shear stress, S is the perimeter over which τ acts, ρ is the phase density and β is the angle of inclination from the horizontal (positive for upward flow). The subscripts L and G denote liquid and gas, respectively; the subscript i denotes interface.

Assuming incompressible flow and combining the two momentum equations by eliminating the pressure terms using the approximate relation

$$P_{iG} - P_{iL} = \sigma \frac{\partial^2 h_L}{\partial x^2}, \quad [5]$$

where σ is the surface tension, yields the following 3 equations:

$$\frac{\partial h_L}{\partial t} + \frac{A_L}{A'_L} \frac{\partial U_L}{\partial x} + U_L \frac{\partial h_L}{\partial x} = 0, \quad [6]$$

$$\frac{\partial h_L}{\partial t} - \frac{A_G}{A'_L} \frac{\partial U_G}{\partial x} + U_G \frac{\partial h_L}{\partial x} = 0 \quad [7]$$

and

$$\rho_L \frac{\partial U_L}{\partial t} - \rho_G \frac{\partial U_G}{\partial t} + \rho_L U_L \frac{\partial U_L}{\partial x} - \rho_G U_G \frac{\partial U_G}{\partial x} + (\rho_L - \rho_G) g \cos \beta \frac{\partial h_L}{\partial x} - \sigma \frac{\partial^3 h_L}{\partial x^3} = F, \quad [8]$$

where

$$F = -\frac{\tau_L S_L}{A_L} + \frac{\tau_G S_G}{A_G} + \tau_i S_i \left(\frac{1}{A_L} + \frac{1}{A_G} \right) - (\rho_L - \rho_G) g \sin \beta \quad [9]$$

and A'_L is dA_L/dh_L .

A linearization procedure, which follows the general approach presented by Barnea & Taitel (1989), yields

$$\begin{aligned} \frac{A}{A'_L} \sigma \frac{\partial^4 \hat{h}_L}{\partial x^4} + \left[\frac{\rho_L U_L^2}{R_L} + \frac{\rho_G U_G^2}{R_G} - (\rho_L - \rho_G) g \cos \beta \frac{A}{A'_L} \right] \frac{\partial^2 \hat{h}_L}{\partial x^2} + 2 \left[\frac{\rho_L U_L}{R_L} + \frac{\rho_G U_G}{R_G} \right] \frac{\partial^2 \hat{h}_L}{\partial t \partial x} \\ + \left[\frac{\rho_L}{R_L} + \frac{\rho_G}{R_G} \right] \frac{\partial^2 \hat{h}_L}{\partial t^2} = \left[-\frac{A}{A'_L} \frac{\partial F}{\partial h_L} - \frac{U_G}{R_G} \frac{\partial F}{\partial U_G} + \frac{U_L}{R_L} \frac{\partial F}{\partial U_L} \right] \frac{\partial \hat{h}_L}{\partial x} + \left[-\frac{1}{R_G} \frac{\partial F}{\partial U_G} + \frac{1}{R_L} \frac{\partial F}{\partial U_L} \right] \frac{\partial \hat{h}_L}{\partial t}, \quad [10] \end{aligned}$$

where \hat{h}_L is the perturbed liquid level and R is the phase holdup. Note that, all the terms in the square brackets in [10] are evaluated at the steady state (unlike these terms in [1]–[9], where these values are the local transient values).

Substituting for the perturbed liquid level,

$$\hat{h}_L = \epsilon e^{i(\omega t - kx)}, \quad [11]$$

into [10] yields the following dispersion equation for the angular frequency, ω :

$$\omega^2 - 2(ak - bi)\omega + ck^2 - dk^4 - eki = 0, \quad [12]$$

where

$$a = \frac{1}{\rho} \left(\frac{\rho_L U_L}{R_L} + \frac{\rho_G U_G}{R_G} \right) \quad [13a]$$

$$b = \frac{1}{2\rho} \left[\left(\frac{\partial F}{\partial U_{LS}} \right)_{U_{GS}, R_L} - \left(\frac{\partial F}{\partial U_{GS}} \right)_{U_{LS}, R_L} \right] \quad [13b]$$

$$c = \frac{1}{\rho} \left(\frac{\rho_L U_L^2}{R_L} + \frac{\rho_G U_G^2}{R_G} - (\rho_L - \rho_G) g \cos \beta \frac{A}{A'_L} \right) \quad [13c]$$

$$d = \frac{\sigma A}{\rho A'_L} \quad [13d]$$

$$e = -\frac{1}{\rho} \left(\frac{\partial F}{\partial R_L} \right)_{U_{LS}, U_{GS}} \quad [13e]$$

and

$$\rho = \frac{\rho_L}{R_L} + \frac{\rho_G}{R_G}. \quad [13f]$$

The solution for ω is

$$\omega = (ak - bi) \pm \sqrt{(a^2 - c)k^2 - b^2 + dk^4 + (ek - 2abk)i}. \quad [14]$$

The steady-state solution is unstable whenever the imaginary part of ω in [14], namely ω_1 , is negative, leading to exponential growth of the perturbed variable, \hat{h}_1 . The amplification factor is $-\omega_1$.

For the case of inviscid flow, a simple expression for ω is obtained:

$$C \equiv \frac{\omega}{k} = \frac{\frac{\rho_L U_L}{H_L} + \frac{\rho_G U_G}{H_G}}{\frac{\rho_L}{H_L} + \frac{\rho_G}{H_G}} \pm \sqrt{\frac{(\rho_L - \rho_G)g}{\frac{\rho_L}{H_L} + \frac{\rho_G}{H_G}} - \frac{\frac{\rho_L \rho_G}{H_L H_G} (U_G - U_L)^2}{\left(\frac{\rho_L}{H_L} + \frac{\rho_G}{H_G} \right)^2} + \frac{\sigma k^2}{\frac{\rho_L}{H_L} + \frac{\rho_G}{H_G}}}, \quad [15]$$

where $H_L = A_L/A'_L$ and $H_G = A_G/A'_G$; C is the wave velocity and k is the wavenumber. As long as the term in the square root is positive, the amplification factor in this case is 0. When the square root is negative, two conjugate solutions for the imaginary parts exist. The second solution, namely the one with the negative sign, is the one that contributes to the instability.

For the viscous case, the solution for ω can be expressed conveniently in a polar form:

$$\omega_1 = (ak - bi) + \sqrt[4]{\alpha^2 + \gamma^2} \exp \left[i \frac{1}{2} \arctan \left(\frac{\gamma}{\alpha} \right) \right] \quad [16a]$$

and

$$\omega_2 = (ak - bi) + \sqrt[4]{\alpha^2 + \gamma^2} \exp \left\{ i \frac{1}{2} \left[\arctan \left(\frac{\gamma}{\alpha} \right) + 2\pi \right] \right\} \quad [16b]$$

where $\alpha = (a^2 - c)k^2 + dk^4 - b^2$ and $\gamma = ek - 2abk$. The negative value of the imaginary part of [16a, b] is the amplification factor.

The condition for marginal stability can be obtained from [12] for the special case where ω_1 , the imaginary part, equals 0. This leads to the following stability criterion for the viscous case:

$$\left(\frac{e}{2b} - a \right)^2 - (a^2 - c) - dk^2 < 0. \quad [17]$$

Substituting the value of $a^2 - c$ from [13] into [17] yields

$$(C_V - C_{IV})^2 + \frac{\rho_L \rho_G}{\rho^2 R_L R_G} (U_G - U_L)^2 - \frac{\rho_L - \rho_G}{\rho} g \cos \beta \frac{A}{A'_L} - \frac{\sigma A}{\rho A'_L} k^2 < 0. \quad [18]$$

The last three terms on the LHS of [18] can be observed as the well-known KH instability of the interface of one-dimensional flow with no viscous effects on the stability. The first term is the additional effect of the shear stresses, which tends to amplify any disturbance in the film thickness. Note that the fourth term, which is the contribution of the surface tension, is the only term that depends on the wavelength. For long waves this term approach zero and it does not affect the neutral stability criterion that should apply to all wavelengths.

The critical wave velocity on the inception of instability, C_V , obtained from [12] for $\omega_1 = 0$, equals ($e/2b$):

$$C_V = \frac{e}{2b} = \frac{\left(\frac{\partial F}{\partial R_L}\right)_{U_{LS}, U_{GS}}}{\left[\left(\frac{\partial F}{\partial U_{GS}}\right)_{U_{LS}, R_L} - \left(\frac{\partial F}{\partial U_{LS}}\right)_{U_{GS}, R_L}\right]} \tag{19}$$

The dispersion equation for the IKH analysis is obtained from [12] with $e = 0$ and $b = 0$. The critical wave velocity in this case, C_{IV} , is equal to [13a], namely:

$$C_{IV} = a = \frac{\rho_L U_L R_G + \rho_G U_G R_L}{\rho_L R_G + \rho_G R_L} \tag{20}$$

Thus, the first term in the KH stability criterion [17], that results from considering the shear stresses, is related to the difference between the wave velocity obtained from the VKH theory and the wave velocity for the inviscid case, on the inception of instability.

In this work the shear stress τ_L , τ_G and τ_i are evaluated as follows:

$$\tau_L = f_L \frac{\rho_L U_L^2}{2} \tag{21}$$

$$\tau_G = f_G \frac{\rho_G U_G^2}{2} \tag{22}$$

and

$$\tau_i = f_i \frac{\rho_G (U_G - U_L) |U_G - U_L|}{2} \tag{23}$$

where

$$f_L = C_L \left(\frac{D_L U_L}{\nu_L}\right)^{-n} \tag{24a}$$

and

$$f_G = C_G \left(\frac{D_G U_G}{\nu_G}\right)^{-m} \tag{24b}$$

D_L and D_G are the hydraulic diameters, evaluated in the following manner:

$$D_L = \frac{4A_L}{S_L} \tag{25a}$$

and

$$D_G = \frac{4A_G}{S_G + S_i} \tag{25b}$$

The coefficients C_G and C_L equal 0.046 for turbulent flow and 16 for laminar flow, n and m take the values of 0.2 for turbulent flow and 1.0 for laminar flow. The interfacial friction factor was assumed to have a constant value of $f_i = 0.014$, as suggested by Cohen & Hanratty (1968) for stratified wavy flow, or $f_i = f_G$ when $f_G > 0.014$.

RESULTS AND DISCUSSION

Figure 1 compares the results of the neutral stability criterion for stratified flow obtained by the VKH analysis [18] and the IKH approach ([18] without the first term). The calculations were made for the case of air-liquid (of water density) in a 5 cm horizontal pipe. It can be seen that for low viscosities the IKH analysis overpredicts considerably the viscous results. However, as the liquid viscosity increases the contribution of the term $(C_v - C_{1V})^2$ in [18] diminishes and for high viscosity both approaches yield almost the same results.

The fact that the results obtained by the VKH analysis, which takes into account the shear stresses, are different from those using the IKH approach at low viscosities, while the two approaches yield almost the same results at high viscosities is indeed puzzling.

In order to see the reason for this anomaly, we consider the behavior of the amplification factor at various flow conditions, as obtained by the two analyses.

The rate of amplification is examined along line a-b in figure 1. Point (a) is the intersection point with the VKH neutral stability curve, while point (b) is the intersection with the IKH neutral stability curve.

The dispersion equation [12] yields two solutions for ω_1 . Positive or zero solutions indicate stable flow. For the VKH analysis, ω_{11} is always positive, while ω_{12} changes sign from positive (stable flow) below point (a) to negative (unstable flow) for U_{LS} above point (a). For the IKH analysis, ω_{11} and ω_{12} are zero for U_{LS} below point (b). Above point (b) ω_{12} is negative (unstable) and ω_{11} is the positive conjugate solution for ω_{12} . The value of $-\omega_{12}$ is the rate of amplification of the disturbance and is illustrated in figure 2 as a function of the wavelength, for a constant gas flow rate ($U_{GS} = 5$ m/s) and at various liquid flow rates (along line a-b in figure 1). The results obtained for the two analyses (VKH and IKH) are almost the same and the results of the solutions are indistinguishable in this figure (although the neutral stability criterion is quite different). A scaled-up picture of the two solutions is shown in figure 3 to show the behavior at low amplification rates. In this figure the details around the conditions of neutral stability can be seen. For liquid flow rates below point (a) ($U_{LS} = 0.1$ m/s), $-\omega_{12}$ is negative for all wavelengths according to the VKH analysis, namely the flow is stable. For U_{LS} between points (a) and (b), $0.15 < U_{LS} < 0.6$ m/s, $-\omega_{12}$ is positive with very low absolute values and only at $U_{LS} = 0.6$ m/s, where the flow becomes unstable also according to the inviscid analysis, does the rate of amplification become meaningful. Stated differently, under the flow conditions where the IKH analysis indicates a zero rate of amplification, the VKH analysis yields a transition from a negative to a positive value of $-\omega_{12}$ with absolute values that are close to zero. Only at conditions where the IKH analysis indicates unstable flow is the rate of amplification obtained by the VKH analysis substantial.

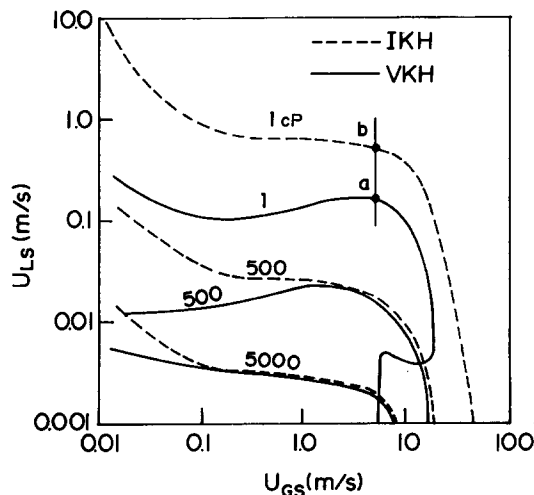


Figure 1. Effect of liquid viscosity on the VKH and IKH neutral stability criteria. Air-liquid, atmospheric pressure, horizontal pipe, $D = 5$ cm.

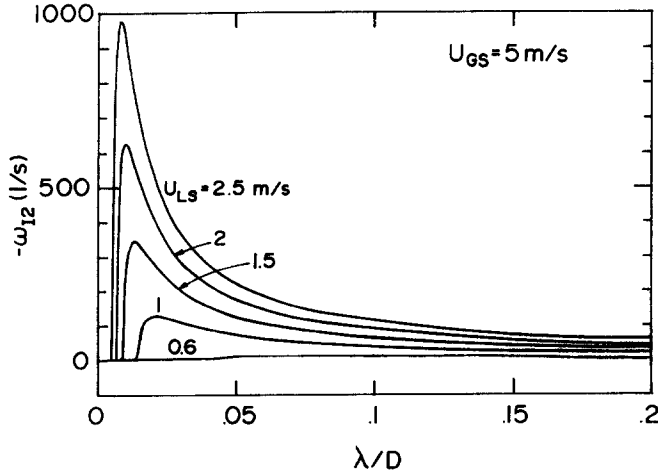


Figure 2. Amplification factor for air-water at $U_{GS} = 5$ m/s.

A convenient method for comparing the amplification factor of the two solutions with respect to the flow rates is to look at the amplification factor at a certain wavelength. This wavelength may be chosen arbitrarily. In this work we chose to compare the solutions at the wavelength which yields the maximum rate of amplification. Figure 4 shows the maximal rate of amplification at each liquid flow rate for a constant gas flow rate. The results are given for a wide range of liquid viscosities. It can be clearly seen, again, that from this point of view the stability behavior of the system is almost the same according to the two KH analyses. For each liquid viscosity under consideration both analyses yield almost the same results and the amplification factor for the IKH analysis is, again, indistinguishable from that for the VKH analysis. A careful examination reveals, however, that there are differences which are only apparent at a very low amplification factor.

For the inviscid case the amplification factor is exactly zero up to the point where the liquid velocity is sufficiently large and the amplification curve maintains a clearly visible positive slope. This is the neutral stability point for the IKH analysis. The behavior of the amplification factor for the VKH analysis, although it looks the same in figure 4, is however different. It is not zero for a low liquid flow rate but rather it is negative for a very low liquid flow rate and becomes positive for an increasing liquid flow rate. The point where the amplification factor changes sign is the neutral stability point for the VKH analysis. This fact cannot be observed in figure 4, since in the region of changing sign the amplification factor is very small and very close to zero. Therefore the results for the VKH analysis look the same as those for the IKH analysis. This point of neutral stability

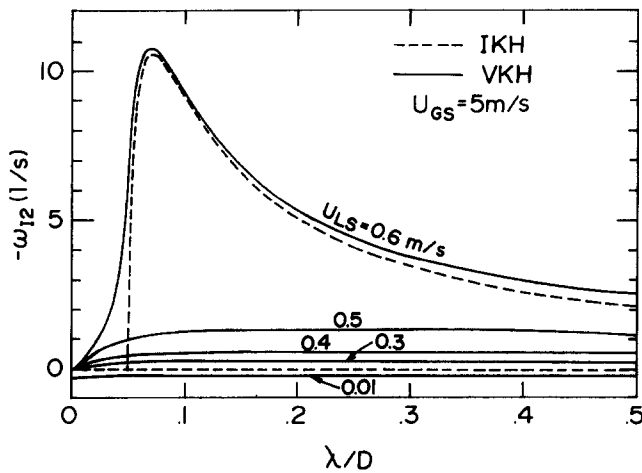


Figure 3. Scale-up amplification factor for air-water at $U_{GS} = 5$ m/s.

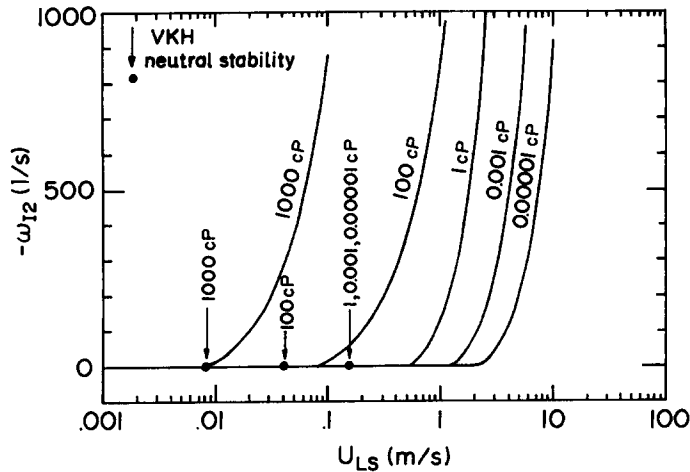


Figure 4. Effect of liquid viscosity on the amplification factor, $U_{GS} = 5$ m/s. Air-liquid, atmospheric pressure, horizontal pipe, $D = 5$ cm.

due to the VKH analysis is designated by arrows in figure 4. For example, for a viscosity of 100 cP the neutral VKH point is at $U_{LS} \approx 0.04$ m/s, whereas the IKH neutral stability point is at 0.08 m/s. Thus, although the general behavior of the IKH and VKH analyses is similar with respect to the value of the amplification factor, they behave differently near the zero amplification factor. As a result, the neutral stability point for the IKH and VKH analyses is not the same.

An interesting point to observe is the effect of viscosity on the location of the neutral stability points. One would expect that as the viscosity decreases the VKH analysis would approach the IKH results. Indeed, for low viscosity, the amplification factor for the low liquid flow rate approaches the zero value, as in the IKH analysis. But at the same time, the exact point of changing sign, i.e. the neutral stability point, moves to the "left" compared to the IKH neutral stability point. On the other hand, for high viscosities the two neutral points are at almost the same location. Thus (see figure 4), the neutral stability point for 1000 cP for both cases is at $U_{LS} \approx 0.008$ m/s. For 100 cP the neutral stability points are at $U_{LS} \approx 0.04$ and 0.08 m/s. For viscosity < 1 cP, the VKH neutral stability point stays at $U_{LS} \approx 0.15$ m/s, while the IKH neutral stability point moves to a higher liquid flow rate as the viscosity decreases. Thus, it is clearly seen that the neutral stability points for the VKH and IKH analyses are farther apart for low viscosity than for high viscosity, giving the impression that the IKH analysis is similar to the VKH analysis for high viscosity but not for low viscosity.

Physical Interpretation

The physical interpretation of the results of the aforementioned analysis is not at all straightforward. The key question is how to interpret the behavior in the unstable regions due to both the IKH and VKH analyses. Do these instabilities result in a transition to slug flow, annular flow or just cause the interface to be wavy?!

As is well-known, the IKH instability does not predict well the transition boundary from stratified flow. The stable region predicted by the IKH analysis is larger compared with the experimental data. As a result, a few attempts to use this type of analysis required the insertion of some correction factors to account for this discrepancy (Kordyban & Ranov 1970; Taitel & Dukler, 1976; Kordyban 1977; Mishima & Ishii 1980).

Lin & Hanratty (1986), Wu *et al.* (1987) and Crowley *et al.* (1992) used the VKH analysis for the prediction of the transition boundaries from stratified flow and found good agreement with the data for the case of a low void fraction. On the other hand, Hanratty (1983) and Andreussi *et al.* (1985) indicated that the VKH analysis can be used successfully to explain the transition to roll waves for the case of a thin liquid level: namely, the unstable infinitesimal wave grows, due to this instability to a large-amplitude wave of the order of the liquid film (roll waves). Barnea (1991) adopted this general approach and gave a complete quantitative description for the behavior

of the interface in the various unstable regions. It was shown that the neutral stability condition of the VKH analysis is not directly associated with the transition to slug or annular flow but rather to an unstable interface with roll waves. Whenever the liquid supply in the film is large enough ($h_L/D > 0.5$) to provide the liquid needed to bridge the pipe, the unstable region becomes slug flow. For $h_L/D < 0.5$, either roll waves or annular flow may exist. In order to obtain annular flow, the upper part of the pipe should be wetted also under conditions of high void (low liquid level). It occurs when the suction effect of the pressure generated over the wave by the Bernoulli effect overcomes the stabilizing influence of gravity. This effect is in phase with the wave height and grows unboundedly until the upper part is wetted. Barnea (1991) suggested that since this description is consistent with the IKH analysis, it is suggested that the IKH analysis is also valid when the waves become finite.

Thus, two regions of instability are identified. The region bounded between the VKH and IKH neutral stability lines and the region "outside" the IKH neutral stability curve. The first region is associated with large-amplitude roll waves for $h_L/D < 0.5$ and slug flow for $h_L/D > 0.5$. For the region outside the IKH neutral stability line the IKH instability will result in either slug flow for $h_L/D > 0.5$ or annular flow for $h_L/D < 0.5$.

The present work supports this general explanation. It further identifies the region between the VKH and IKH neutral stability lines with the region of low amplification factor. Within this region the Bernoulli effect is small and the instability is caused by the viscous effect (the two first term in [18]). In this case the amplification factor is of a lower order which does not lead to an unbounded growth. On the other hand, the region of IKH instability is associated with very high amplification factor (by both analyses), which results in exponential growth that always leads to the transition from stratified flow.

Referring now to figure 5, the zone bounded by the VKH neutral stability curve is a zone of stable stratified flow (stratified smooth or stratified with small-amplitude waves). The region between the VKH (—) and the IKH (---) curves is a region of either roll waves or slug flow. The curve $h_L/D = 0.5$, is a dividing line between slug flow to the "left" and large-amplitude roll waves to the "right". At a relatively high liquid rate these large-amplitude waves were termed pseudo-slug (Lin & Hanratty 1987), wavy annular (Barnea *et al.* 1980) or proto-slug (Nicholson *et al.* 1987). At a low liquid flow rate this is a transitional region to annular flow (which was identified as wavy by some researchers and as annular by others). The region outside the IKH curve is either in slug flow, for the region $h_D/D > 0.5$, or annular flow, for the region where $h_L/D < 0.5$. Thus, a complete behavior is determined by three demarcation lines: the neutral VKH line, the neutral IKH line and the curve $h_L/D = 0.5$. Note again that the IKH neutral stability line is at the same location as where the VKH analysis shows a sharp increase in the amplification factor. Thus, along line a-b, the flow changes from stable stratified flow to large-amplitude roll waves (usually referred to as wavy annular, proto- or pseudo-slug in this region) and then above $h_L/D = 0.5$ the flow pattern is slug flow. Along the line c-d, the flow changes from stable stratified flow to annular flow through a narrow region of large-amplitude waves.

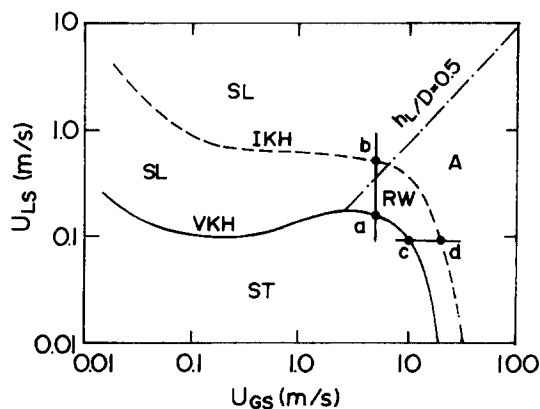


Figure 5. Flow pattern prediction by the VKH and IKH analyses. Air-water, atmospheric pressure, horizontal pipe, $D = 5$ cm. SL—slug; ST—stratified; RW—roll waves; A—annular.

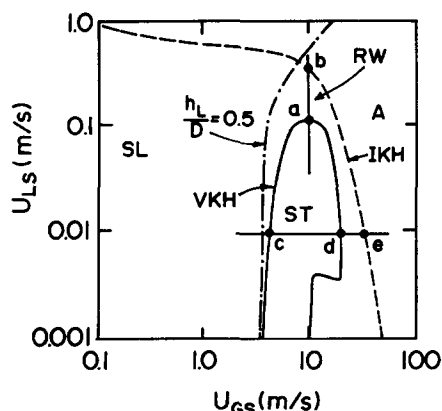


Figure 6. Flow pattern transition boundaries for upwards inclined flow, $\beta = 0.25^\circ$. Air-water, atmospheric pressure, $D = 5$ cm. SL—slug; ST—stratified; RW—roll waves; A—annular.

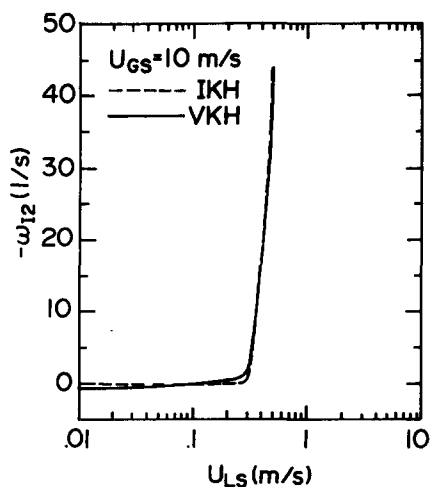


Figure 7. Amplification factor for upwards inclined flow, $U_{Gs} = 10$ m/s. Air-water, atmospheric pressure, $\beta = 0.25^\circ$, $D = 5$ cm.

A similar behavior regarding the stability characteristic of the system is obtained for the case of inclined stratified flow. For upwards inclined flow the stable area predicted by the VKH analysis is bounded by a bell-shaped curve on the U_{Ls} vs U_{Gs} plot (figure 6), while the IKH neutral stability curve shows a totally different behavior. The maximum amplification rates along a constant gas flow rate (line a-b) and along a constant liquid flow rate (line c-d-e) are illustrated in figures 7 and 8, respectively. It is shown again that, although the neutral stability curves obtained by the two analyses are quite different, the amplification curves are very similar. Figure 7 shows how the maximal amplification factor changes along the line a-b. The results are similar to the horizontal case (figure 4). Figure 8 shows the maximal amplification rate for increasing gas flow rate. As can be seen, the amplification factor is positive and small for a low gas flow rate, it becomes negative, i.e. a stable interface, for the region from point c to d and thereafter a sharp increase in the amplification factor is shown where the flow become unstable due to IKH analysis (point e).

Figure 9 is a typical representation of the stability behavior of downward inclined stratified flow. The amplification factor curves for the two analyses yield almost the same results. However, along the region where the IKH analysis predicts zero amplification (namely, neutral stability conditions), the flow is unstable according to the VKH analysis with a very small amplification rate. This means that, for this case, the neutral stability line due to the VKH analysis is absent and the transition

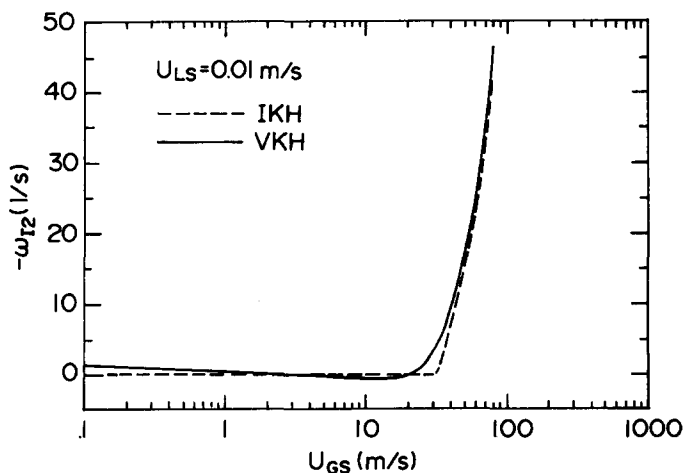


Figure 8. Amplification factor for upwards inclined flow, $U_{Ls} = 0.01$ m/s. Air-water, atmospheric pressure, $\beta = 0.25^\circ$, $D = 5$ cm.

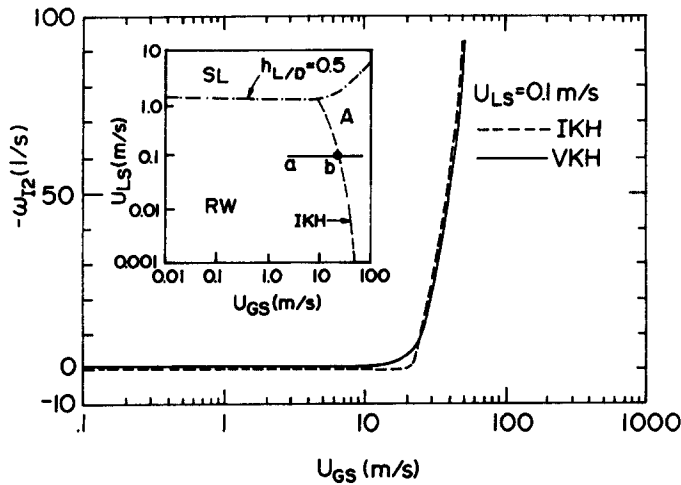


Figure 9. Amplification factor for downwards inclined flow, $U_{LS} = 0.1$ m/s. Air-water, atmospheric pressure, $\beta = -5^\circ$, $D = 5$ cm. SL—slug; ST—stratified; RW—roll waves; A—annular.

from stratified flow is controlled only by the IKH analysis and $h_L/D = 0.5$. The whole region bounded by the aforementioned lines is, therefore, a region of stratified roll waves.

Note that Andritsos & Hanratty (1987), using a two-dimensional, inviscid analysis for a flat geometry, also related the wave type to the amplification factor. This approach and interpretation, however, is quite different from the one presented here.

SUMMARY AND CONCLUSIONS

- (1) This work addresses the dilemma that the neutral stability lines based on the viscous complete two-fluid model equations and the approximate inviscid analysis lead to similar results for high viscosity but quite different results for low liquid viscosity. This fact seems to be unreasonable since one would expect the VKH analysis to approach the IKH case for low viscosity.
- (2) It is shown that the results for the amplification factor based on the IKH and VKH analyses are almost the same.
- (3) For increasing liquid flow rates or increasing gas flow rates the amplification factor for the IKH analysis is zero up to a point, where after it grows very sharply to very high value. This point is the neutral stability point for the IKH analysis.
- (4) In the range where the IKH analysis predicts zero amplification, the VKH analysis predicts a very low amplification factor. This amplification factor can be positive (unstable) or negative (stable). The transition from negative to positive amplification is the neutral stability line for the VKH analysis.
- (5) In spite of the fact that the general behavior for the amplification factor for the VKH and IKH analysis is similar and that the sharp increase in amplification factor occurs almost at the same conditions, the neutral stability points are quite different for low viscosity fluids.
- (6) The results obtained in this analysis confirm the interpretation of Barnea (1991). The region of low amplification, i.e. the region between the neutral stability line of the VKH analysis and that of the IKH analysis, is a region of roll waves or slug flow (depending on the liquid holdup). The region of high amplification, i.e. the region above the IKH neutral stability line is a region where the flow will be either slug or annular.

REFERENCES

- ANDREUSSI, P., ASALI, J. C. & HANRATTY, T. J. 1985 Initiation of roll waves in gas-liquid flows. *AIChE JI* **31**, 119-126.
- ANDRITSOS, N. & HANRATTY, T. J. 1987 Interfacial instability for horizontal gas-liquid flows in pipelines. *Int. J. Multiphase Flow* **13**, 583-603.

- ANDRITSOS, N., WILLIAMS, L. & HANRATTY, T. J. 1989 Effect of liquid viscosity on the stratified-slug transition in horizontal pipe flow. *Int. J. Multiphase Flow* **15**, 877–892.
- BARNEA, D. 1991. On the effect of viscosity on stability of stratified gas liquid flow—application to flow pattern transition at various pipe inclination. *Chem. Engng Sci. J.* **46**, 2123–2131.
- BARNEA, D. & TAITEL, Y. 1989 Transient formulation modes and stability of steady state annular flow. *Chem. Engng Sci* **44**, 325–332.
- BARNEA, D., SHOHAM, O., TAITEL, Y. & DUKLER, A. E. 1980 Flow pattern transition for gas-liquid flow in horizontal and inclined pipes. Comparison of experimental data with theory. *Int. J. Multiphase Flow* **6**, 217–226.
- COHEN, S. L. & HANRATTY, T. J. 1968 Effects of waves at a gas-liquid interface on a turbulent air flow. *J. Fluid Mech.* **31**, 467–469.
- CROWLEY, C. J., WALLIS, G. B. & BARRY, J. J. 1992 Validation of a one-dimensional wave model for the stratified to slug flow regime transition, with consequences for wave growth and slug frequency. *Int. J. Multiphase Flow* **18**, 249–271.
- HANRATTY, T. J. 1983 Interfacial instabilities caused by air flow over a thin liquid layer. In *Waves on Fluid Interfaces*, pp. 221–259. Academic Press, New York.
- LIN, P. Y. & HANRATTY, T. J. 1986 Prediction of the initiation of slugs with linear stability theory. *Int. J. Multiphase Flow* **12**, 79–98.
- LIN, P. Y. & HANRATTY, T. J. 1987 Effect of pipe diameter on the interfacial configurations for air-water flow in horizontal pipes. *Int. J. Multiphase Flow* **13**, 549–563.
- KORDYBAN, E. S. 1977 Some characteristics of high waves in closed channels approaching Kelvin-Helmholtz instability. *ASME JI Fluids Engng* **99**, 339–346.
- KORDYBAN, E. S. & RANOV, T. 1970 Mechanism of slug formation in horizontal two-phase flow. *J. Bas. Engng* **92**, 857–864.
- MISHIMA, K. & ISHII, M. 1980 Theoretical prediction of onset of horizontal slug flow. *ASME JI Fluids Engng* **102**, 441–445.
- NICHOLSON, M. K., AZIZ, K. & GREGORY, G. A. 1978 Intermittent two phase flow in horizontal pipes: predictive models. *Can. J. Chem. Engng* **56**, 653–663.
- TAITEL, Y. & DUKLER, A. E. 1976 A model for prediction of flow regime transitions in horizontal and near horizontal gas-liquid flow. *AIChE JI* **22**, 47–55.
- WALLIS, G. B. 1969 *One-dimensional Two-phase Flow*. McGraw-Hill, New York.
- WU, H. L., POTS, B. F. M., HOLLENBERG, J. F. & MEERHOFF, R. 1987 Flow pattern transitions in two-phase gas/condensate flow at high pressure in an 8-inch horizontal pipe. In *Proc. 3rd Int. Conf. on Multi-Phase Flow*, The Hague, The Netherlands, pp. 13–21.